

A novel blind adaptive algorithm applied to new designed smart antenna array for interference suppression

Saeed Komeylian^a, Majid Tayarani^{a,*}, Seyed Hassan Sedighy^b

^aDepartment of Electrical Engineering, Iran University of Science and Technology, Tehran 16846-13114, Iran

^bSchool of New Technologies, Iran University of Science and Technology, Tehran 16846-13114, Iran

(Communicated by Seyed Hossein Siadati)

Abstract

In this study, a novel blind adaptive algorithm with discrete periodic variables is introduced. The proposed discrete periodic variable algorithm (DPVA) has been applied to the new designed 7-element antenna array. The DPVA is based on minimizing the output power to steer null (or nearly null) gain in the direction of interference. Discrete phase shift leads to the use of hybrid phase shifter in practice and thus reduction of implementation costs. In addition, the proposed algorithm has low computational complexity. Results show that DPVA has fast and reliable convergence. It is converged within less than 400 iterations and less than 1 millisecond time duration. The null depth created by this algorithm is 90 dB which is an indication of pure cancellation of the interference. Furthermore, the effect of a number of interference sources is investigated. It is shown that the null depth is decreased by the increase of interference sources. In the studied 7-element array, increasing the interference sources up to 6 decreases the null depth to 20 dB.

Keywords: Optimization, Blind adaptive algorithm, Discrete phase shift, Beamforming, Smart antenna
2020 MSC: 62F35, 74K10

1 Introduction

GNSS receiver antenna is designed to receive signals in desired direction and at special frequency range. However, existence of noise, interference and multi-path fading, deteriorate the antenna performance. Since the interference operating frequency is the same as the desired GNSS signal, it is not possible to use the conventional filtering method. As a result, spatial filtering with array of antenna has received a great deal of attention [5, 6, 11, 16]. Spatial filtering or beamforming is a process that place the low gain in the direction of the interference by weighting and summing the signals from each separated antenna in the array. For optimal processing, a common method is minimizing the mean output power of the array. This is due to the fact that interference power level is much higher than electromagnetic wave and noise power. An adaptive algorithm is required to adjust the weights for each antenna due to variable location of interferences relative to the antenna array [2, 15, 17, 23]. If the location of interferences and also other spatial knowledge are not specified and thus training sequence is not available, the algorithm is known as blind adaptive algorithm [8, 10].

*Corresponding author

Email addresses: sepas720@gmail.com (Saeed Komeylian), majid@Tayarani.com (Majid Tayarani), sedighy@iust.ac.ir (Seyed Hassan Sedighy)

The most important advantage of blind adaptive algorithm is that they are more stable, and also independent of channel properties and array calibration [4]. However, blind algorithms have generally more slowly convergence comparing to training sequence-based algorithms. Hence, it is important to identify existing algorithms and introduce more reliable and faster convergence algorithms.

The decision directed approach (DDA) is a common method of blind adaptive algorithm. In this approach, the output is demodulated and the estimated symbols are known as training sequence. This method needs carrier synchronization which is difficult and motivate researchers to use algorithms such as CMA [2].

One of the most common blind adaptive algorithm is constant modulus algorithm (CMA) which has a constant envelope [2]. In this algorithm the weighting coefficient in each iteration improved by summation of previous stage coefficient with defined step. CMA was first used by Godard, Treichler and Agee as least mean square type [1, 9, 20]. The drawback was slow convergence rate. Using nonlinear least squares by [1, 19] as LS-CMS improved the convergence rate. Gross [10] has introduced LMS and RLS algorithms. Both algorithms have high side-lobe level but different convergence rate. LMS method has low convergence rate and RLS has medium convergence rate. HW-CMA and HW-LS-CMA have been proposed by Dakulagi [4]. Theses algorithms improved CMA by reducing side-lobe level. The HW-CMA improved the rate of convergence by using adaptive step size for beamforming. The HW-LS-CMA applied Hanning window to the weight coefficient and reduced the side-lobe level.

In this study, a new blind adaptive algorithm is proposed based on discrete signal phase shift, despite of the most other existing algorithms. In practice, a hybrid phase shifter is used for discrete phase shift which reduces the computation and implementation cost. The performance of the proposed DPVA algorithm has been investigated on the new designed antenna array with 7 separate antennas. The effect of number of interference sources and also null depth in the direction of the interference has been evaluated. Details of the proposed algorithm and its simulation results on the antenna array are described in the following sections.

2 Basis of the problem and mathematical formulation

Figure 1 shows the array of antenna with M elements which is placed in the environment with L desirable electromagnetic wave signals, K interference and also noise sources ($\mathbf{s}(f)$, $\mathbf{q}(f)$ and $\mathbf{n}(f)$, respectively). Array consists of same antennas. However, due to mutual coupling effect, there is a slight difference in the performance of the antennas and as a result each one has unique radiation pattern. The antenna radiation pattern implies that at each angle of arrival (AOA) which amount of signal is received.

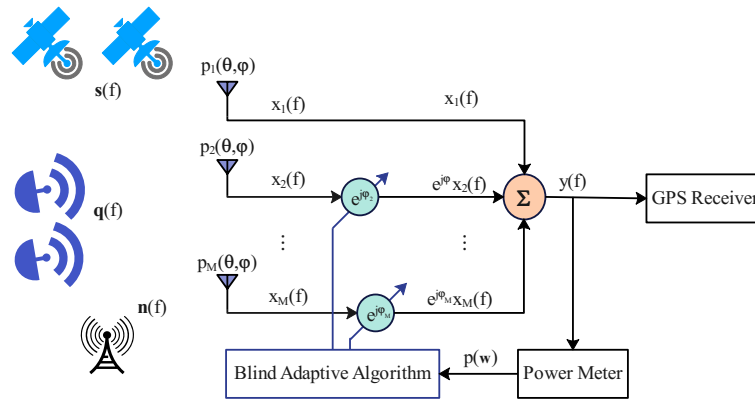


Figure 1: Frequency Domain

L desirable signal source vector is defined as (2.1).

$$\mathbf{s}(f) \triangleq \begin{bmatrix} s_1(f) \\ s_2(f) \\ \vdots \\ s_L(f) \end{bmatrix} \quad (2.1)$$

K interference source vector is implied as (2.2).

$$\mathbf{q}(f) \triangleq \begin{bmatrix} q_1(f) \\ q_2(f) \\ \vdots \\ q_K(f) \end{bmatrix} \quad (2.2)$$

As illustrated in Figure 1 the radiation pattern of i^{th} antenna is stated as $p_i(\theta, \varphi)$. Hence the antenna array radiation pattern vector represent as $\mathbf{p}(\theta, \varphi)$ is defined by (2.3).

$$\mathbf{p}(\theta, \varphi) = \begin{bmatrix} p_1(\theta, \varphi) \\ p_2(\theta, \varphi) \\ \vdots \\ p_M(\theta, \varphi) \end{bmatrix} \quad (2.3)$$

Product of $p_i(\theta_h, \varphi_h)$ in $h(f)$, where $h(f)$ is an arbitrary electromagnetic wave arrived from $(\theta, \varphi) = (\theta_h, \varphi_h)$, is equal to the received signal from i^{th} antenna ($x_i(f)$). It is written as (2.4).

$$x(f) = p_i(\theta, \varphi)h(f) \quad (2.4)$$

Consequently, the signal received by an antenna from $s_i(f)$ at AOA of (θ_i, φ_i) is defined as (2.5)

$$\mathbf{x}_s(f) = \sum_{i=1}^L p(\theta_i, \varphi_i)s_i(f) \quad (2.5)$$

Similarly \mathbf{x}_q is implied as (2.6), where (θ'_j, φ'_j) represents AOA of $q_j(f)$.

$$\mathbf{x}_q(f) = \sum_{j=1}^K p(\theta'_j, \varphi'_j)q_j(f) \quad (2.6)$$

$n_i(f)$ is the noise received from i^{th} antenna. The received noise vector is defined as (2.7)

$$\mathbf{x}_n(f) = \begin{bmatrix} n_1(f) \\ n_2(f) \\ \vdots \\ n_M(f) \end{bmatrix} \quad (2.7)$$

The total received signal is obtained by summation of the $\mathbf{x}_s(f)$, $\mathbf{x}_q(f)$ and $\mathbf{x}_n(f)$. This is stated in (2.8) and (2.9)

$$\mathbf{x}(f) = \mathbf{x}_s(f) + \mathbf{x}_q(f) + \mathbf{x}_n(f) = \sum_{i=1}^L \mathbf{p}(\theta_i, \varphi_i)s_i(f) + \sum_{j=1}^K \mathbf{p}(\theta'_j, \varphi'_j)q_j(f) + \mathbf{n}(f) \quad (2.8)$$

$$\mathbf{x}(f) = \mathbf{P}_s \mathbf{s}(f) + \mathbf{P}_q \mathbf{q}(f) + \mathbf{n}(f) \quad (2.9)$$

Where \mathbf{P}_s matrix is defined as (2.10).

$$\mathbf{P}_s \triangleq \begin{bmatrix} p_1(\theta_1, \varphi_1) & p_1(\theta_2, \varphi_2) & \cdots & p_1(\theta_L, \varphi_L) \\ p_2(\theta_1, \varphi_1) & p_2(\theta_2, \varphi_2) & \cdots & p_2(\theta_L, \varphi_L) \\ \vdots & \vdots & \ddots & \vdots \\ p_M(\theta_1, \varphi_1) & p_M(\theta_2, \varphi_2) & \cdots & p_M(\theta_L, \varphi_L) \end{bmatrix} \quad (2.10)$$

Similarly, \mathbf{P}_q matrix is stated as (2.11).

$$\mathbf{P}_q \triangleq \begin{bmatrix} p_1(\theta'_1, \varphi'_1) & p_1(\theta'_2, \varphi'_2) & \cdots & p_1(\theta'_K, \varphi'_K) \\ p_2(\theta'_1, \varphi'_1) & p_2(\theta'_2, \varphi'_2) & \cdots & p_2(\theta'_K, \varphi'_K) \\ \vdots & \vdots & \ddots & \vdots \\ p_M(\theta'_1, \varphi'_1) & p_M(\theta'_2, \varphi'_2) & \cdots & p_M(\theta'_K, \varphi'_K) \end{bmatrix} \quad (2.11)$$

In the Beamforming process, a null is placed in the direction of interference by appropriate weighting of the received signals from each antenna. This is stated by product of weighting factor in received signal. The weighted received signal, interference and noise are described in (2.12), (2.13) and (2.14), respectively.

$$\mathbf{x}_{s_w}(f) = \begin{bmatrix} w_1 x_{s_1}(f) \\ w_2 x_{s_2}(f) \\ \vdots \\ w_m x_{s_M}(f) \end{bmatrix} \quad (2.12)$$

$$\mathbf{x}_{q_w}(f) = \begin{bmatrix} w_1 x_{q_1}(f) \\ w_2 x_{q_2}(f) \\ \vdots \\ w_M x_{q_M}(f) \end{bmatrix} \quad (2.13)$$

$$\mathbf{x}_{n_w}(f) = \begin{bmatrix} w_1 x_{n_1}(f) \\ w_2 x_{n_2}(f) \\ \vdots \\ w_M x_{n_M}(f) \end{bmatrix} \quad (2.14)$$

Where w_i is defined as (2.15) and the weighing coefficient vector $\mathbf{w}(f)$ is implied as (2.16).

$$w_i = e^{-j\tau_i(2\pi f)} \quad (2.15)$$

$$\mathbf{w}(f) = \begin{bmatrix} 1 \\ e^{-j\tau_2(2\pi f)} \\ \vdots \\ e^{-j\tau_M(2\pi f)} \end{bmatrix} \quad (2.16)$$

In this investigation, the power minimization method is used to create null in the direction of interference. Total power is defined as $\mathbf{E}\{y\}$ where $\mathbf{E}\{\cdot\}$ denotes the expectation operator. Mathematical explanation of total power is shown in (2.17) and (2.18).

$$y(f) = \mathbf{w}^t (\mathbf{x}_s(f) + \mathbf{x}_q(f) + \mathbf{x}_n(f)) \quad (2.17)$$

$$p(\mathbf{w}) = E \{y(f)\} = E \{ \mathbf{w}^t (\mathbf{x}_s(f) + \mathbf{x}_q(f) + \mathbf{x}_n(f)) \} \quad (2.18)$$

Because all signals include desired, interference and noise are uncorrelated and each one has zero mean, the equation (2.18) can be written as (2.19).

$$p(\mathbf{w}) = E \{ \mathbf{w}^t \mathbf{x}_s(f) \} + E \{ \mathbf{w}^t \mathbf{x}_q(f) \} + E \{ \mathbf{w}^t \mathbf{x}_n(f) \} = p_s(\mathbf{w}) + p_q(\mathbf{w}) + p_n(\mathbf{w}) \quad (2.19)$$

As shown in (2.20) and (2.21), The power of desired signal is less than noise significantly. However, the noise power is less than the interference power.

$$p_s(\mathbf{w}) \ll p_n(\mathbf{w}) \quad (2.20)$$

$$p_n(\mathbf{w}) \ll p_q(\mathbf{w}) \tag{2.21}$$

So, with a good estimation, the total power can be written as (2.22).

$$p(\mathbf{w}) \approx p_q(\mathbf{w}) \tag{2.22}$$

From above equations, it is clear that minimizing the total power leads to eliminate of interference. In the next section, details of the proposed algorithm for power minimization is explained.

3 Proposed blind adaptive algorithm

As described in previous sections, in this investigation the beamforming is applied by appropriate weighting and summation of the arrival signals from each antenna to eliminate the interference effect. Finally, the goal function to be minimized is the power of the antenna array ($p(\mathbf{w})$). In this investigation, a threshold power (p_{th}) of $0.5 W$ is set and minimum power should be less than p_{th} . The weighting coefficient vector \mathbf{w} is implied as (3.1). Also, the equation of power is described in (3.2).

$$\mathbf{w} \triangleq \begin{bmatrix} w_1 \\ w_2 \\ w_3 \\ \vdots \\ w_M \end{bmatrix} \tag{3.1}$$

$$p(\mathbf{w}) = E \left\{ \sum_{i=1}^M w_i x_i(f) \right\} \tag{3.2}$$

In practice, weighting is applied by phase shift of arrival signals with a p-bit hybrid phase shifter. A P-bit phase shifter with 360 degrees of monotonic phase coverage, has a least significant bit (LSB) of $\frac{2\pi}{2^p}$ radian. In frequency domain, the signal weighting coefficient is a factor of $e^{j\frac{2\pi}{2^p}}$. It means that w_i is a member of periodic geometric sequence (PGS) with first term of 1 and common ratio of $\frac{2\pi}{2^p}$ as implied in (3.3).

$$1, e^{j\frac{2\pi}{2^p}}, e^{j\frac{4\pi}{2^p}}, e^{j\frac{6\pi}{2^p}}, e^{j\frac{8\pi}{2^p}}, \dots, e^{j\frac{2^p-1\pi}{2^p}}, e^{j\frac{2^p\pi}{2^p}}, e^{j\frac{2^p+1\pi}{2^p}}, \dots \tag{3.3}$$

Thus w_i is represented by (3.4).

$$\begin{cases} w_i = 1 & i = 1 \\ w_i \in \left\{ 1, e^{j\frac{2\pi}{2^p}}, e^{j\frac{4\pi}{2^p}}, e^{j\frac{6\pi}{2^p}}, e^{j\frac{8\pi}{2^p}}, \dots, e^{j\frac{(2^p-1)2\pi}{2^p}} \right\} & i = 2 \text{ to } M \end{cases} \tag{3.4}$$

In this study, common ratio of 2^p -PGS ($e^{j\frac{2\pi}{2^p}}$) is called phase shift step (PSS). As shown in Figure 2(a) each term of PGS is generated by multiplying previous term by PSS. As an example, for 2-bit phase shifter demonstrated in Figure 2(b), w_i is selected from 1,j,-1,-j.

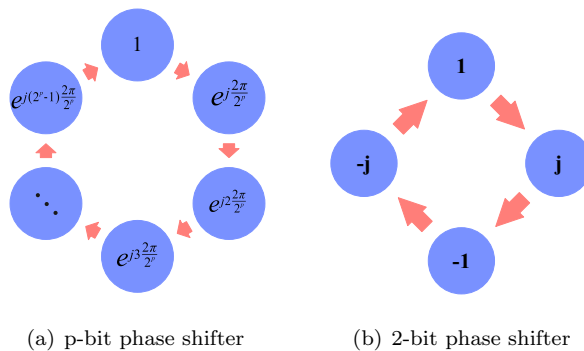


Figure 2: Elements of weighting coefficient vector

Hence, due to properties mentioned above, the proposed algorithm is named Discrete Periodic Variable Algorithm (DPVA). In the first step of DPVA, a unit random vector (\mathbf{w}_{rand}) is set with elements randomly selected from (3.4). In the next step, a sequence of improved approximations to the minimum is generated, each derived from the preceding approximation. Thus if \mathbf{w}_j is the approximation to the minimum obtained in the j^{th} iteration, the improved approximation in the $(j + 1)^{th}$ iteration is found from (3.5):

$$\mathbf{w}_{j+1} = \mathbf{u}(PSS, b, c)\mathbf{w}_j \tag{3.5}$$

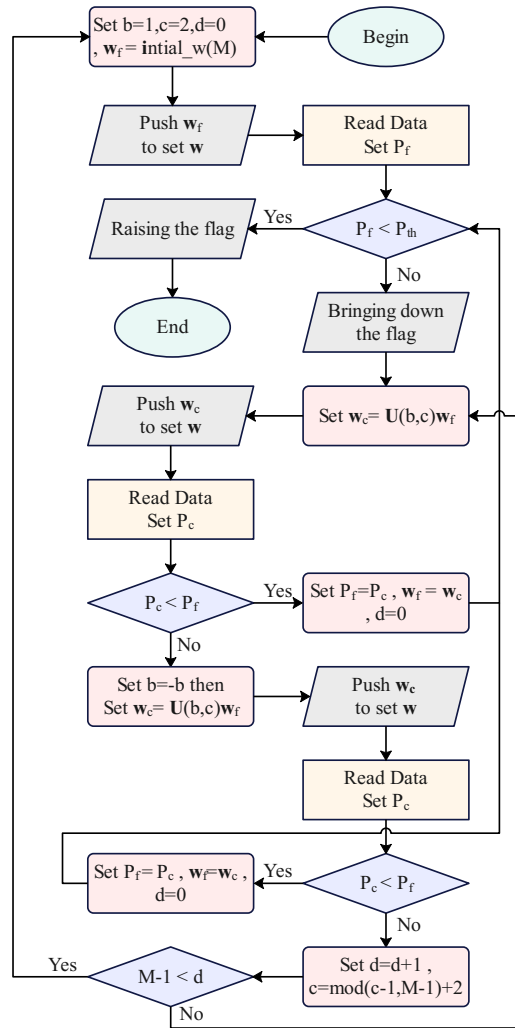


Figure 3: DPVA flowchart

$\mathbf{U}(PSS, b, c)$ is a $M \times M$ matrix as a function of PSS, b and c parameter. $\mathbf{U}(PSS, b, c)$ operator multiply PSS^b by c^{th} element of \mathbf{w}_j . The b parameter has two values, +1 and -1. In fact, if the phase shift increase of \mathbf{w}_c does not lead to power minimization, the phase shift decrease should be checked and this is done by applying the b parameter. The c parameter implies which antenna coefficient is being evaluated. For c^{th} element of weighting coefficient vector, if the power is not decreased by increase or decrease of phase shift, the existed \mathbf{w}_j is the elected weighting coefficient which leads to minimum power referenced to c^{th} element. By increasing the c number, the next element of weighting coefficient vector is verified and this is continued since $c=M$. If $M-1$ elements of \mathbf{w}_j vector are not changed sequentially, the local minimum power is obtained. When the power value is larger than threshold power, a new random vector (\mathbf{w}_{rand}) has to set and mentioned process should be repeated. The flowcharts of DPVA is clarified in Figure 3 and 4. The difference between these figures is that Figure 4 is nonstop. Because in practice, the antenna array should cancel the interference, continuously. A schematic of tending to minimized power by DPVA is demonstrated in Figure 5.

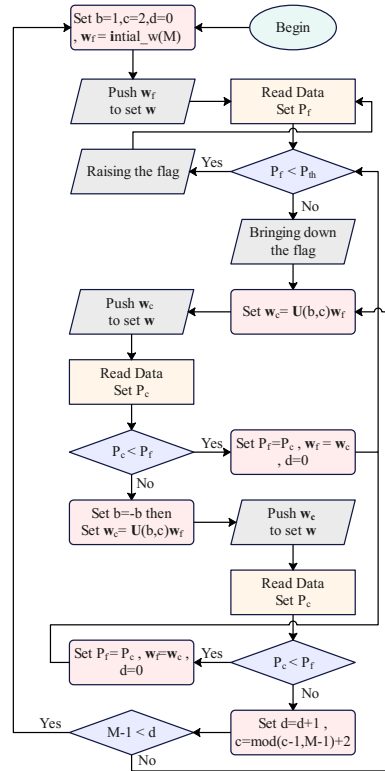


Figure 4: Nonstop DPVA flowchart

The mathematical explanation of DPVA is explained in the following. The matrix \mathbf{Q} , as a function of M and independent from b and c , is defined as relation (3.6) .

$$\mathbf{Q} \triangleq \begin{bmatrix} 0 & \mathbf{Z}_{1 \times (M-2)} & 0 \\ 0 & \mathbf{Z}_{1 \times (M-2)} & 1 \\ \mathbf{Z}_{(M-2) \times 1} & \mathbf{I}_{(M-2) \times (M-2)} & \mathbf{Z}_{(M-2) \times 1} \end{bmatrix} \quad (3.6)$$

The \mathbf{Q} operator is applied on an arbitrary vector \mathbf{g} as (3.7)

$$\mathbf{k} \triangleq \mathbf{Q}\mathbf{g} \quad (3.7)$$

It can be easily shown that $\mathbf{k}_2 = \mathbf{g}_M$, $\mathbf{k}_1 = 0$ and for j between 2 and $M-1$, $\mathbf{k}_{j+1} = \mathbf{g}_j$. In other words, the product of the matrix \mathbf{Q} in each vector, zeros the first term of matrix and other terms are shifted by one unit, circularly . The \mathbf{I} matrix is defined as (3.8).

$$\mathbf{l}(b) \triangleq \begin{bmatrix} \mathbf{Z}_{(M-2) \times 1} \\ \sqrt{e^{j \frac{b\pi}{2^{p-1}}} - 1} \\ 0 \end{bmatrix} \quad (3.8)$$

As described above, product of \mathbf{Q} in $\mathbf{l}(\mathbf{Q}\mathbf{l})$ make a vector with M^{th} element of $\sqrt{e^{j \frac{b\pi}{2^{p-1}}} - 1}$ and zero term for all other elements. $\mathbf{Q}^2\mathbf{l}(b) = \mathbf{Q}(\mathbf{Q}\mathbf{l}(b))$ is also a vector whose elements are all zero except for the second element, which has a value of $\sqrt{e^{j \frac{b\pi}{2^{p-1}}} - 1}$. So in general, the vector \mathbf{h} in terms of \mathbf{Q} and \mathbf{l} is stated as (3.9) .

$$\mathbf{h}(b, c) \triangleq \mathbf{Q}^c\mathbf{l}(b) \quad (3.9)$$

As explained above, \mathbf{h} is a vector whose elements are all zero except for the c^{th} element with value of $\sqrt{e^{j \frac{b\pi}{2^{p-1}}} - 1}$. The matrix $\mathbf{U}(PSS, b, c)$ is defined as relation (3.10).

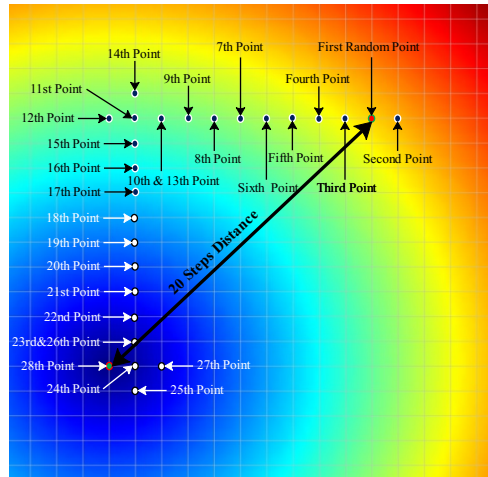


Figure 5: Power minimization path with DPVA

$$\mathbf{U}(PSS, b, c) \triangleq \mathbf{I}_{M \times M} + \mathbf{h}(b, c)\mathbf{h}^T(b, c) \tag{3.10}$$

In above equation, $\mathbf{h}(b, c)\mathbf{h}^T(b, c)$ is a square matrix, all of which are zero except for (c, c) element with value of $e^{j\frac{b\pi}{2^p-1}} - 1$. Thus $U(PSS, b, c)$ is the same as the matrix \mathbf{I} , with the different (c, c) element which is equal to $e^{j\frac{b\pi}{2^p-1}}$. Consequently, the product of matrix $U(PSS, b, c)$ in each vector just changes the c^{th} element value and multiplying it by $e^{j\frac{b\pi}{2^p-1}}$.

4 Simulation result

The DPVA is applied to the new designed antenna array. Array consists of 7 GNSS antenna operate at frequency range of 1.575-1.602 with circular polarization. Figure 6 illustrates the arrangement of antennas in the array.

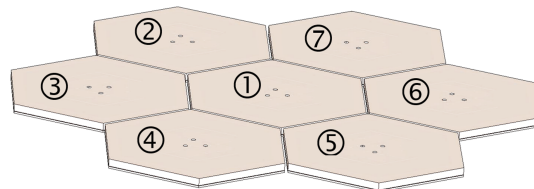


Figure 6: Antenna array

A threshold of $0.5 W$ is set for output power. The convergence behavior of the proposed algorithm is evaluated in terms of normalized output power referenced to p_{th} versus iteration and time duration. As it is clearly shown in Figure 7, the proposed algorithm is converged with less than 400 iterations which counts as a good number for discrete phase shift algorithms.

One of the main parameters in the performance of algorithms is computation complexity and accordingly, the convergence time duration. This is a crucial feature due to rapid change of environment condition in current problem. Therefore, the complexity of computations between different algorithms is compared in Table 1.

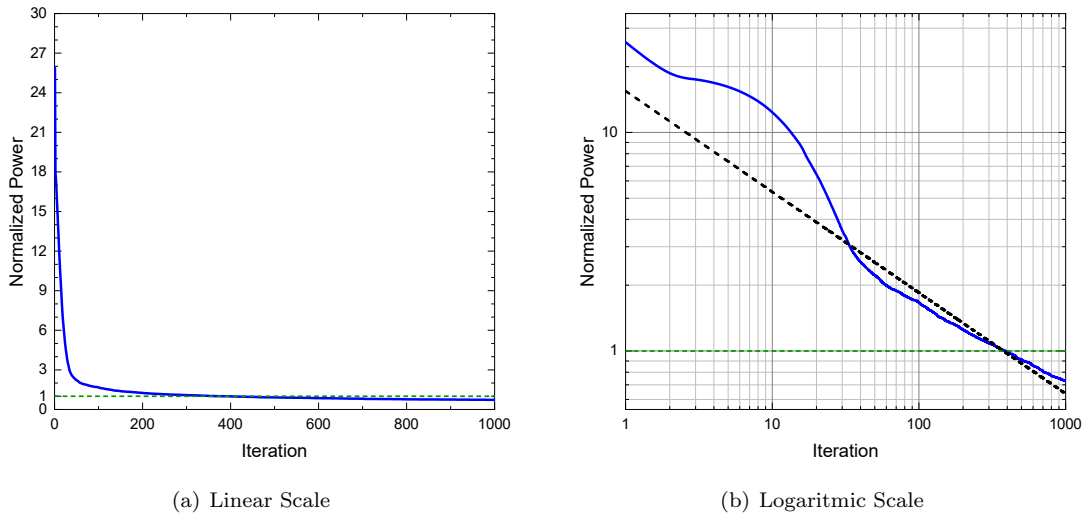


Figure 7: Convergence behavior

Table 1: The comparison of computational complexity in different algorithms

Algorithm	Number of multiplies	Number of pluses
Structured WLCCM-KS-RLS [22]	$36M^2 + 71M + 55$	$32M^2 + 56M + 15$
Direct WLCCM-KS-RLS [22]	$72M^2 + 62M + 43$	$64M^2 + 42M + 12$
WL-AVF [18]	$120M^2 + 128M + 12$	$120M^2 + 96M - 12$
LCCM-KS-RLS [22]	$18M^2 + 43M + 122$	$16M^2 + 37M + 4M + 98$
L-AVF [18]	$30M^2 + 60M + 12$	$28M^2 + 48M - 12$
Blind GVFF [3]	$12M^2 - 12M + 3$	$5M^2 - 8M + 5$
Proposed algorithm (DPVA)	M^2	$M^2 + M - 1$

As can be seen, the proposed method (DPVA) reduces the computational complexity. The convergence speed is evaluated by using generate code of MATLAB for $M=8$ and $p=4$. The convergence time of DPVA is less than 1 millisecond, while according to the articles [23], time interval of interference location changes is considered as 200 milliseconds. Consequently, the proposed algorithm is able to follow all interference sources and cancel them. Another effective parameter of interference suppression algorithms is null depth in the interference direction. In Table 2, the number of array elements and the null depth in different algorithms are compared. As clearly shown, DPVA with a null depth of 90 dB has the best interference suppression performance.

Table 2: The comparison of null depth in different algorithms

Algorithm	No. of array elements	Null depth in the direction of interference (dB)
LMS [21]	8	20.6
SMI [13]	8	22.2
RLS [14]	8	23.6
Conventional STAP [7]	8	50
Improved STAP [12]	8	78
Proposed algorithm (DPVA)	7	90

An array with N elements is able to remove $N-1$ interference signals. In this study the array consists of 7 elements and thus the effect of one to six interference sources in different directions has been investigated. In Table 3, the hypothetical direction of interference signals is determined. Furthermore, the necessary phase shift value for each antenna is calculated by applying the DPVA. As can be seen, discrete shifting is performed in 0.1 degrees step increment which leads to use a 12-bit phase shifter in practice.

Table 3: Location of interference sources and required phase shift for interference cancellation

Number of interference source	Location of the interference source (θ, φ)	Phase shift calculated from the proposed algorithm						
		Antenna						
		1	2	3	4	5	6	7
1	$(10^\circ, 330^\circ)$	0	172.9	359.9	359.9	359.9	5	359.9
2	$(10^\circ, 330^\circ), (20^\circ, 180^\circ)$	0	191	359.9	159.8	12.3	110.2	205.8
3	$(10^\circ, 330^\circ), (20^\circ, 180^\circ), (30^\circ, 30^\circ)$	0	241.3	43.2	160	294.7	7	139
4	$(10^\circ, 330^\circ), (20^\circ, 180^\circ), (30^\circ, 30^\circ), (45^\circ, 90^\circ)$	0	127.2	263.3	26	69.9	160.5	272.5
5	$(10^\circ, 330^\circ), (20^\circ, 180^\circ), (30^\circ, 30^\circ), (45^\circ, 90^\circ), (60^\circ, 270^\circ)$	0	90.2	182.1	336	94.9	227.8	312
6	$(10^\circ, 330^\circ), (20^\circ, 180^\circ), (30^\circ, 30^\circ), (45^\circ, 90^\circ), (60^\circ, 270^\circ), (80^\circ, 120^\circ)$	0	88.6	169.1	314.1	83.5	235.3	322.6

To check the performance of the array in removing the interference, the radiation RHCP pattern of the antenna array after applying the weighting on each element is shown in Figure 8. As illustrated, the DPVA is able to create a null gain with an appropriate depth in the interference direction. Results demonstrates that increasing the number of interference sources, decreases the null depth. Because by increasing the interference source count, the optimization algorithm must satisfy more conditions with fixed number of equations. This is clearly shown in Figure 9 which compares the null depth for different number of interference sources.

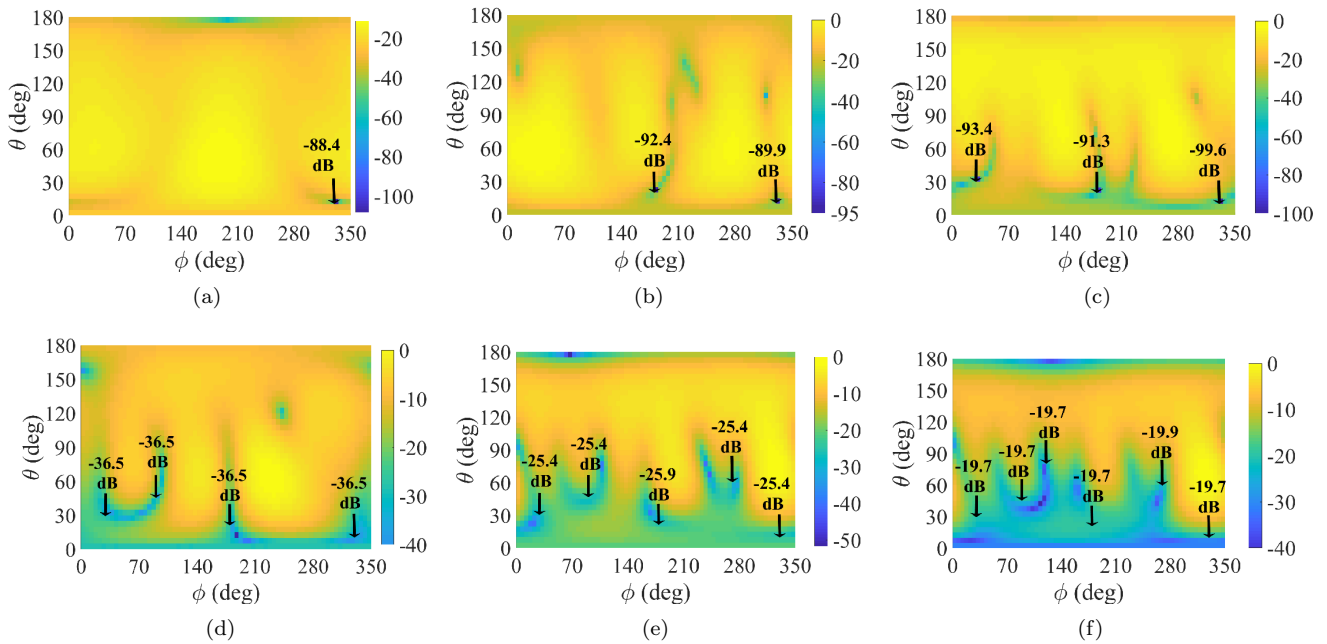


Figure 8: Right hand circular polarization for array of antenna; (a) to (e):1 to 6 interference source count

5 Conclusion

A new blind adaptive algorithm with discrete periodic variable (DPVA) is introduced to eliminate the interference received by GNSS array of antenna. The DPVA is applied to the new-designed array with 7 elements. Numerical simulation has been done to validate the algorithm performance by evaluating RHCP radiation pattern of the array. Furthermore, interference source count is increased from 1 to 6. The following results are obtained:

- The proposed algorithm has reliable convergence behavior. It is converged within less than 400 iterations. Run duration is less than 1 millisecond and in practice it is lower than this amount due to cancellation of some mathematical process such as creating matrix of data.

- The null depth in the direction of interference is 90 dB which implies a desirable ability of interference elimination.

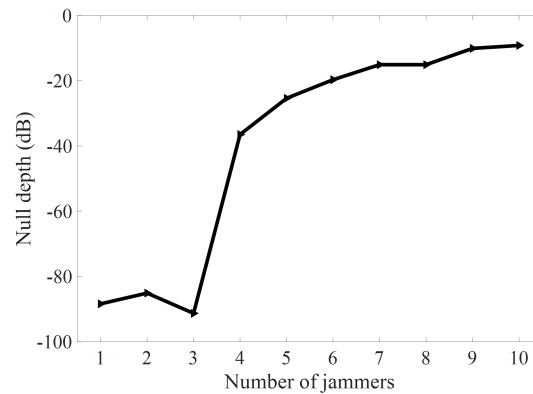


Figure 9: Effect of the number of interference sources on the null depth

-Results denote that increasing the number of interference source decreases the null depth, while it is reached 20 dB for 6 interference sources.

References

- [1] B. Agee, *The least-squares CMA: A new technique for rapid correction of constant modulus signals*, ICASSP '86. IEEE Int. Conf. Acoustics Speech Signal Process., vol. 11, Institute of Electrical and Electronics Engineers, 1986, pp. 953–956.
- [2] T. Biedka, *Analysis and development of blind adaptive beamforming algorithms*, Ph.D. thesis, Faculty of the Virginia Polytechnic Institute and State University, 2001.
- [3] Y. Cai, R.C. de Lamare, M. Zhao, and J. Zhong, *Low-complexity variable forgetting factor mechanism for blind adaptive constrained constant modulus algorithms*, IEEE Int. Conf. Acoustics Speech Signal Process., IEEE, March 2012, pp. 3293–3296.
- [4] V. Dakulagi and M. Bakhar, *Efficient blind beamforming algorithms for phased array and MIMO RADAR*, IETE J. Res. **64** (2018), no. 2, 241–246.
- [5] S. Daneshmand, A. Jahromi, A. Broumandan, and G. Lachapelle, *GNSS space-time interference mitigation and attitude determination in the presence of interference signals*, Sensors **15** (2015), no. 6, 12180–12204.
- [6] D.S. De Lorenzo, Sh.C. Lo, P.K. Enge, and J. Rife, *Calibrating adaptive antenna arrays for high-integrity GPS*, GPS Solutions **16** (2012), no. 2, 221–230.
- [7] R. Ebrahimi and S.R. Seydnejad, *Elimination of pre-steering delays in space-time broadband beamforming using frequency domain constraints*, IEEE Commun. Lett. **17** (2013), no. 4, 769–772.
- [8] L. Ch. Godara, *Smart Antennas*, CRC Press, 2004.
- [9] D. Godard, *Self-recovering equalization and carrier tracking in two-dimensional data communication systems*, IEEE Trans. Commun. **28** (1980), no. 11, 1867–1875.
- [10] F.B. Gross, *Smart Antennas for Wireless Communications with Matlab*, McGraw-Hill Professional, 2005.
- [11] I.J. Gupta, I.M. Weiss, and A.W. Morrison, *Desired features of adaptive antenna arrays for GNSS receivers*, Proc. IEEE **104** (2016), no. 6, 1195–1206.
- [12] D. Li, J. Liu, J. Zhao, G. Wu, and X. Zhao, *An improved space-time joint anti-jamming algorithm based on variable step LMS*, Tsinghua Sci. Technol. **22** (2017), no. 5, 520–528.
- [13] J. Litva and T. Kwok-Yeung Lo, *Digital Beamforming in Wireless Communications*, Artech House, Inc., 1996.
- [14] R. Martínez, A. Del Cacho, L. De Haro, and M. Calvo, *Comparative study of LMS and RLS adaptive-algorithms in the optimum combining of uplink W-CDMA*, IEEE Vehicul. Technol. Conf. **56** (2002), no. 4, 2258–2262.
- [15] A.S.M. Sayem, R.B.V.B. Simorangkir, K.P. Esselle, A. Lalbakhsh, D.R. Gawade, B. O'Flynn, and J.L. Buckley,

- Flexible and transparent circularly polarized patch antenna for reliable unobtrusive wearable wireless communications*, *Sensors* **22** (2022), no. 3, 1276.
- [16] M. Sgammini, F. Antreich, L. Kurz, M. Meurer, and T.G. Noll, *Blind adaptive beamformer based on orthogonal projections for GNSS*, vol. 2, September 2012, pp. 926–935.
- [17] O. Sharifi-Tehrani, M.F. Sabahi, and M.R. Danaee, *Null broadened–deepened array antenna beamforming for GNSS jamming mitigation in moving platforms*, *ICT Express* **8** (2022), no. 2, 161–165.
- [18] N. Song, J. Steinwandt, L. Wang, R.C. De Lamare, and M. Haardt, *Non-data-aided adaptive beamforming algorithm based on the widely linear auxiliary vector filter*, *ICASSP, IEEE Int. Conf. Acoustics Speech. Signal Process. Proc.*, no. 2, 2011, pp. 2636–2639.
- [19] H.W. Sorenson, *Least-squares estimation: From Gauss to Kalman*, *IEEE Spectrum* **7** (1970), no. 7, 63–68.
- [20] J. Treichler and B. Agee, *A new approach to multipath correction of constant modulus signals*, *IEEE Trans. Acoustics Speech Signal Process.* **31** (1983), no. 2, 459–472.
- [21] B. Widrow, P. Mantey, L. Griffiths, and B. Goode, *Adaptive antenna systems*, *J. Acoustic. Soc. Amer.* **42** (1967), no. 5, 1175–1176.
- [22] X. Wu, Y. Cai, M. Zhao, R.C. de Lamare, and B. Champagne, *Adaptive widely linear constrained constant modulus reduced-rank beamforming*, *IEEE Trans. Aerospace Electronic Syst.* **53** (2017), no. 1, 477–492.
- [23] X. Yang, F. Wang, W. Liu, and F. Chen, *A new blind anti-jamming algorithm based on a novel antenna array design*, *IET Radar Sonar Navig.* **16** (2022), no. 10, 1616–1626.